Design, Development and Analysis of Advanced Airboat Propeller by Using Bamboo Composite Fibre Material

[1]Shaik Azmatullah Rahaman, [2]Dr. S. Selvarajan, [3]Y.N.V.Santosh Kumar
[1]Post Graduate Student, [2]Chief scientist, [3]Assistant Professor [3]Head Of the Department
[1,3]Department of Aerospace Engineering, Nimra Institute of Science and Technology, Ibrahimpatnam-521 456, AP, India.
[2]Council of Scientific and Industrial Research - National Aerospace Laboratories, Bangalore-560 037, India.

Abstract **- The objective of this paper was design, development and analysis of propeller by using a bamboo composite fibre material with contra rotating advance airboat propellers, airboat propeller shows characteristics of its non-aviation usage. The design of a propeller is broad, flattened blade and squared-off tips because the aerodynamic favors a high drag that is useful for slowing an airboat. A simple method of predicting the performance of a propeller is the use of Blade Element Theory. In this method the propeller is divided into a number of independent sections along the length. At each section a force balance is applied involving 2D section lift and drag with the thrust and torque produced by the section. At the same time a balance of axial and angular momentum is applied. This produces a set of nonlinear equations that can be solved by iteration for each blade section. The resulting values of section thrust and torque can be summed to predict the overall performance of the propeller.**

Key Words **- Propeller, Computer Aided Three-Dimensional Interactive Application, Computational Fluid Dynamics Blade Element Theory**

Nomenclature-
B = number of propeller blades
a = Speed of sound, [m/s]
C= Chord [m]
C_D= Drag coefficient
C_L = Lift coefficient
C_P =Power coefficient
C_Q = Torque coefficient
C_T = Thrust coefficient
J = advance ratio parameter
K_T = thrust coefficient,
N = revolutions per minute [RPM]
n = revolutions per second [rps]
Q = torque [in-lb]
r = propeller radius [m]
T = thrust [lb]
ρ = density [slugs/ft3]
η_p = propeller efficiency

I. INTRODUCTION

A. Airboat

The first airboat was built in 1905 in Nova Scotia, Canada. An airboat also known as a fan-boat is a flat-bottom vessel and powered by either an aircraft or automotive engine it is very popular means of transportation, parts of the Indian river, they are used for fishing, hunting and eco-tourism, and in other marshy or shallow areas where a standard inboard or outboard engine with a submerged propeller would be impractical.

Propulsion system for an airboat consists of an engine, propeller, and rudders. Various forms of engines that have been used on airboats include aircraft, automotive, turbine, and small high output aluminum block engines.

Figure 1: Airboat

B. Propeller

A propeller is a type of fan that transmits power by converting rotational motion into thrust. A pressure difference is produced between the forward and rear surfaces of the airfoil-shaped blade, and a fluid (such as air or water) is accelerated behind the blade. Propellers on airboats are operated at speeds below the maximum tip speed. In general the maximum tip speed of a propeller is around 890 feet per second.

C. Bamboo Fibres

It is to develop a natural fibre composite with high mechanical properties and to present it as a new natural and renewable option to reinforce both thermoplastic and thermoset matrices, which fits into the requirements (properties, availability and cost) established in the field of reinforcements for composites.

Figure 2: Technical bamboo fibres used in composite materials

II. EXPERIMENTAL DETAILS

A. Design Methodology

The propeller blade is one of the most complicated parts in the propulsion system, It would take direct effect on the structural intensity，vibration，reliability and life-span. There are many engine failures caused by the problems of shroud design. The coordinate points of NACA 4412 can be generated by using CATIA V5R19 software. Airfoil coordinates are taken from the journal papers, as shown in fig. 3. The blade information data had given in table-1

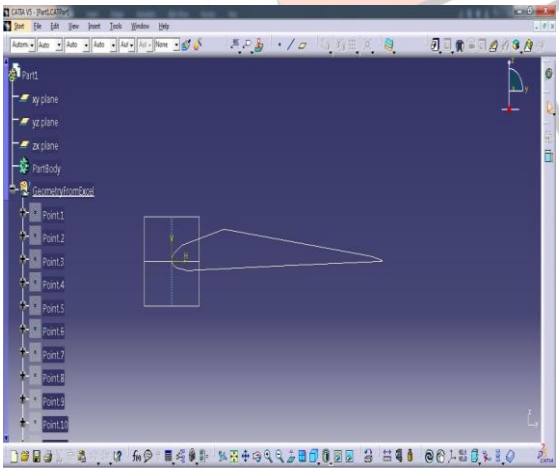

Figure 3: NACA 4412 airfoil

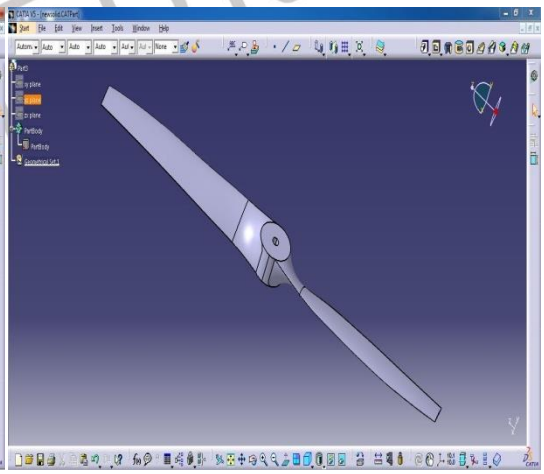

Figure 4: Propeller Blade In part design

Table 1: Blade Information

Propeller diameter [D][m]	**1.2192**
Density [kg/m^3]	1.225
Relative Velocity[m/s]	25
Number of Blades [N_b]	2
Velocity[V] [m/s]	25

A propeller blade can be subdivided into 10 cross section, each cross section is look like an airfoil (as shown in table-2) a discrete number of sections. For each section the flow can be analysed independently if the assumption is made that for each there are only axial and angular velocity components and that the induced flow input from other sections is negligible.

Table 2: Blade geometry

S.NO	AIRFOIL SECTION	X (mm)	Y (mm)	CHORD LINE (mm)	DISTANCE FOR THE HUB (mm)
1	B-B	88.9	54.7878	104.4194	50.8
2	C-C	89.662	50.292	102.7938	112.776
3	D-D	97.028	37.846	104.14	175.006
4	E-E	97.536	28.956	101.7524	236.982
5	F-F	96.012	22.86	98.7044	299.212
6	G-G	94.234	18.542	96.0374	361.188
7	H-H	90.17	15.24	91.44	423.418
8	I-I	82.804	12.7	83.7692	485.394
9	J-J	73.152	10.16	73.8632	547.624
10	K-K	60.452	7.366	60.9092	609.6

B. Computational Fluid Dynamics

Computational fluid dynamics, usually abbreviated as CFD, is a branch of fluid mechanics that uses numerical methods and algorithms to solve and analyze problems that involve fluid flows. Computers are used to perform the calculations required to simulate the interaction of liquids and gases with surfaces defined by boundary conditions.

C. Geometric Modelling

ANSYS ICEM CFD is meant to mesh a geometry are primarily meant to 'clean-up' an imported CAD model. The following is the colour coding in ANSYS ICEM CFD, after the BUILD TOPOLOGY option has been implemented:

1. YELLOW: curve attached to a single surface - possibly a hole exists. In some cases this might be desirable for e.g., thin internal walls require at least one curve with single surface attached to it.
2. RED: curve shared by two surface - the usual case.
3. BLUE: curve shared by more than two surface.
4. Green: Unattached Curves - not attached to any surface.

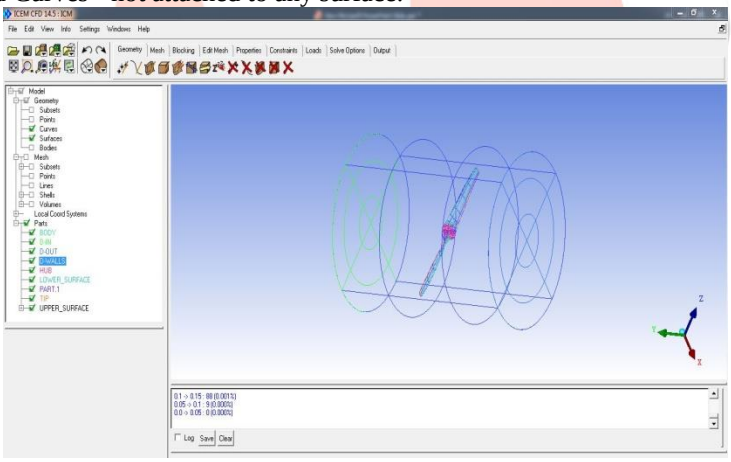

Figure 5: Geometric model of propeller

D. Boundary Conditions

The continuum was chosen as fluid and the properties of air were assigned to it. A moving reference frame is assigned to fluid with a rotational velocity (2800rpm to 10000 rpm). The wall forming the propeller blade and hub were assigned a relative rotational velocity of zero with respect to adjacent cell zone. A uniform velocity 25 m/sec was prescribed at inlet. At outlet outflow boundary condition was set. The far boundary (far field) was taken as inviscid wall and assigned an absolute rotational velocity of zero. Fig. 6 shows the boundary conditions imposed on the propeller domain.

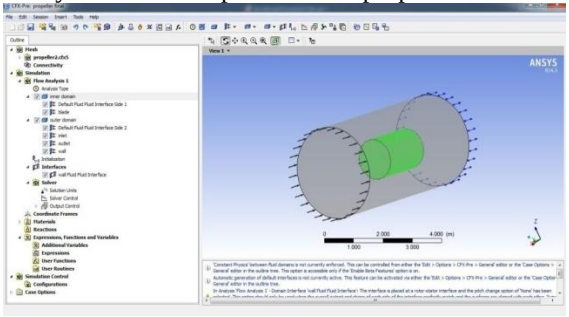

Figure 6: Boundary Conditions on propeller domain

III. RESULTS

The performance of propeller is conventionally represented in terms of non-dimensional coefficients, i.e.

- thrust coefficient (KT),

$$K_T = \frac{T}{\rho n^2 D^4}$$

- torque coefficient (KQ) ,

$$K_Q = \frac{Q}{\rho n^2 D^5}$$

- advance coefficients (J).

$$J = \frac{V_a}{nD}$$

- propeller efficiency and

$$\eta_p = \frac{Tv}{P_{shaft}} = \frac{Tv}{2\pi nQ} \qquad \eta_0 = \frac{J}{2\pi}\frac{K_T}{K_Q}$$

or

A complete computational solution for the flow was obtained using Cfx software. The software also estimated thrust and torque from the computational solutions for different rotational speeds (rps) of the propeller. These were expressed in terms of KT & KQ. The estimated thrust and torques are shown in Table 4. Comparison of estimated non-dimensional coefficients and efficiency (η) against experimental predictions, as obtained from literature, are shown in Table-4. The comparison of predicted KT & KQ with numerical data. It shows that KT and KQ coefficients are decreasing with increasing of advance coefficients (J). Maximum efficiency is observed at J = 0.4572.

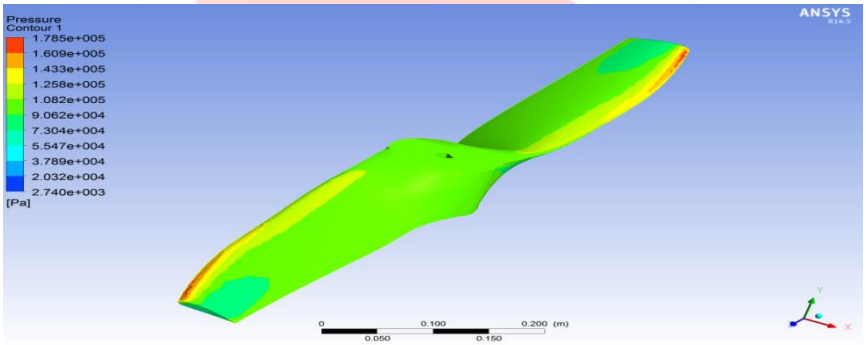

Figure 7: Pressure distribution on the surface of the plane (4000 rpm)

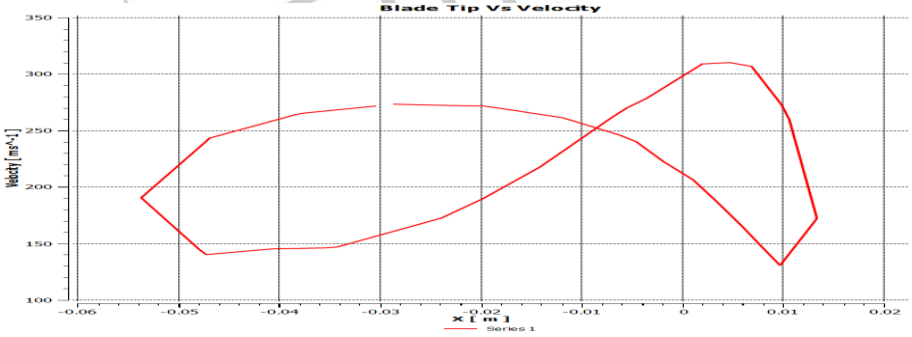

Graph 1: Velocity Distribution over the Tip of the Blade -0.58(M) (4000 Rpm)

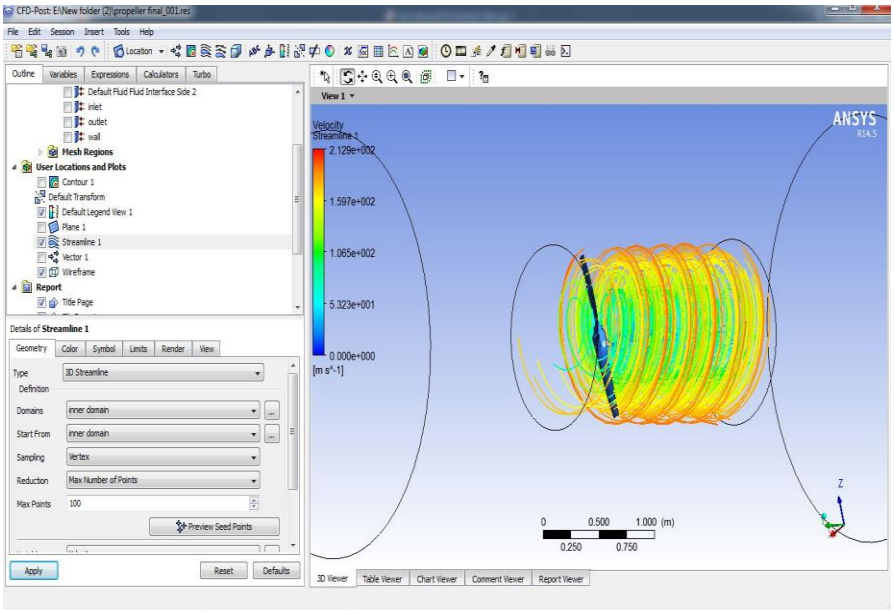

Figure 8: Path Lines at downstream of propeller (4000 rpm)

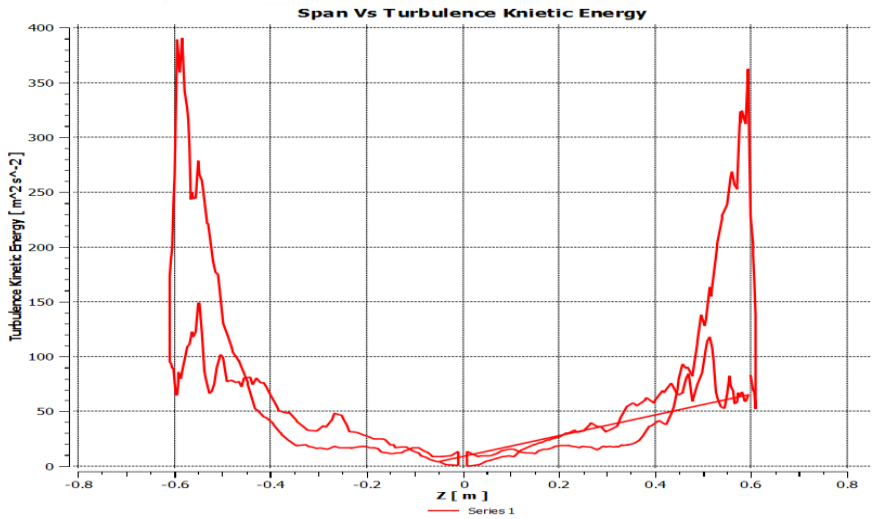

Graph 2: Turbulence Kinetic Energy Distribution over the Blade (4000 Rpm)

Table 3: Total Torque around Blade for Different Rpm

Torque x [Q] [Nm]	Torque y [Q] [Nm]	Torque z [Q] [Nm]	Total Torque[Q] [Nm]
37.4013	0.0322883	37.43609594	86.0583
42.6654	0.0368846	42.70091128	131.889
48.1873	0.0413366	48.22515778	180.394
80.1976	0.0679474	80.26428537	464.598
121.378	**0.071195**	**121.5276527**	**819.128**
131.025	0.0638003	131.2040801	898.59
136.042	0.057171	136.2384426	939.178
141.214	0.0489022	141.4285843	980.765
151.979	0.027282	152.2354243	1065.6
175.335	-0.0426409	175.6934025	1242.21
244.806	-0.35163	245.4511029	1706.68
412.286	-0.39711	412.5606849	2508.83
577.206	-0.29	577.3081396	3138.77
736.354	-0.430704	736.4126557	3765.25
886.274	-0.637828	886.3183913	4304.88
1022.8	-0.84922	1022.882693	4920.22

Table 4: Efficiency Calculation for the Blade for Different Rpm

Propeller rotational Speed [ṅ][rpm]	Propeller rotational Speed [ṅ][rps]	Thrust[T] [N]	Total Torque[Q] [Nm]	Thrust Coefficient [KT]	Torque Coefficient [KQ]	Advance Ratio [J]	Propeller Efficiency [ηProp]
2800	46.66667	1.61338	86.0583	0.0146	0.005209	0.653143	29.15%
2900	48.33333	1.74072	131.889	0.020858	0.005539	0.630621	37.81%
3000	50	1.91004	180.394	0.026659	0.005846	0.6096	44.27%
3500	58.33333	3.27045	464.598	0.050444	0.007148	0.522514	58.72%
4000	**66.66667**	**6.0288**	**819.128**	**0.068092**	**0.008286**	**0.4572**	**59.83%**
4100	68.33333	6.85244	898.59	0.071099	0.008515	0.446049	59.31%
4150	69.16667	7.31329	939.178	0.07253	0.00863	0.440675	58.98%
4200	70	7.7877	980.765	0.073949	0.008746	0.435429	58.62%
4300	71.66667	8.83217	1065.6	0.076652	0.008982	0.425302	57.80%
4500	75	11.2164	1242.21	0.08159	0.009465	0.4064	55.78%
5000	83.33333	17.7804	1706.68	0.090799	0.010711	0.36576	49.37%
6000	100	15.0471	2508.83	0.092691	0.012502	0.3048	35.98%
7000	116.6667	10.8553	3138.77	0.085198	0.012853	0.261257	27.58%
8000	133.3333	9.28443	3765.25	0.078249	0.012553	0.2286	22.69%
9000	150	8.84765	4304.88	0.070688	0.011937	0.2032	19.16%
10000	166.6667	12.9785	4920.22	0.065441	0.011159	0.18288	17.08%

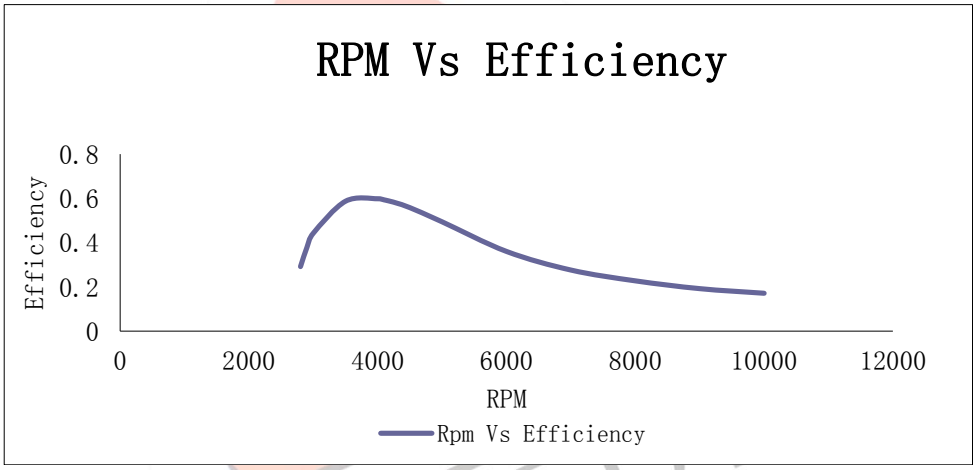

Graph 3: RPM Vs Efficiency

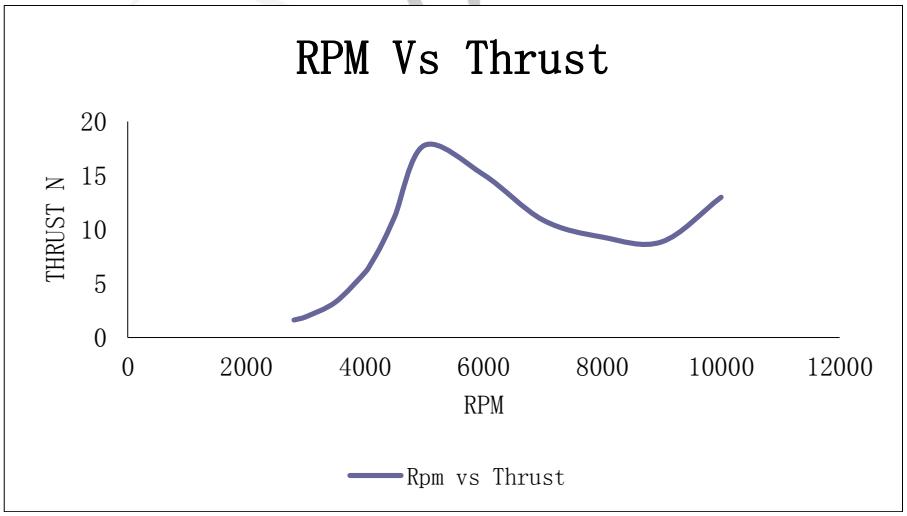

Graph 4: RPM Vs Thrust

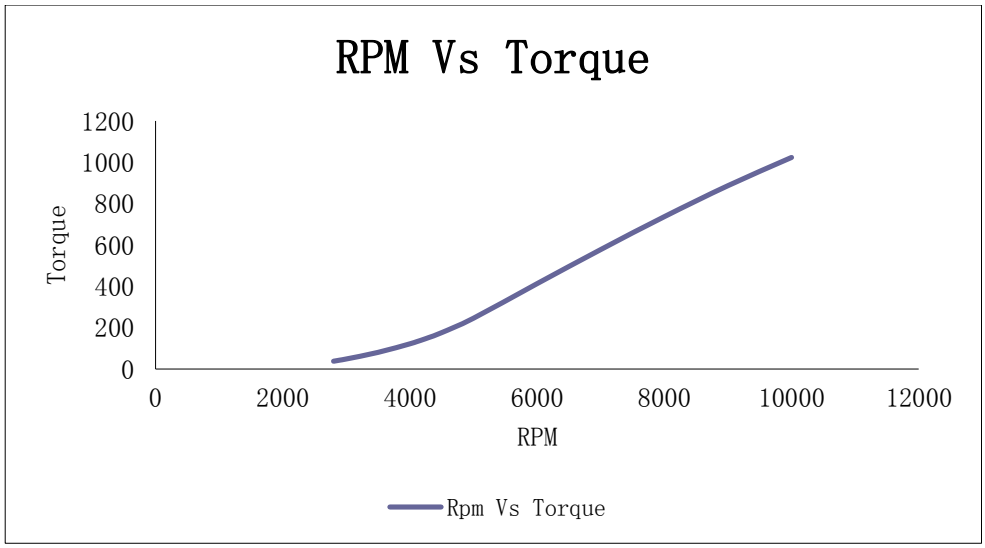

Graph 5: RPM Vs Torque

IV. CONCLUSIONS

From the above analysis and graphs it can be clearly seen that the maximum propeller efficiency is 59.8% (60%). However the maximum efficiency occurs at 4000 rpm itself. This is a lower rpm for a boat application. However, the efficiency has to increase to get better efficiency.

The effort has been taken to optimize the propeller design to get higher efficiency and higher design rpms. The design characteristics has been studied and has been concluded that by changing the overall span of the propeller may increase the thrust. Since the span has been constrained for a particular air boat.

V. ACKNOWLEDGEMENTS

The authors are thankful to The Director and all the scientists of Council of Scientific and Industrial Research - National Aerospace Laboratories, Bangalore for supporting the research work. Also like to thank all the supporting staff of Nimra Institute of Science and Technology, Vijayawada.

VI. REFERENCES

[1] Optimization of an Airboat Design-Adam P. Leppek by Western Michigan University
[2] Blade element and momentum theory. Helis.com. [Online] [Cited: 15 April 2010.] http://www.helis.com/howflies/bet.php.
[3] ANSYS: Introduction to FLUENT. [PDF document] s.l. : ANSYS, Inc. Proprietary, 2009.Salvatore, F., Testa, C., Ianniello, S. and Pereira, F. 2006. Theoretical modeling of unsteady cavitation and induced noise, INSEAN, Italian Ship Model Basin, Rome, Italy, Sixth International Symposium on Cavitation, CAV2006, Wageningen, The Netherlands.
[4] A Three-Equation Eddy-Viscosity Model for Reynolds-Averaged Navier-Stokes Simulations of Transitional Flow," ASME Trans. J. Fluids Eng, 130(12), pp. 121401.1–121401.14.
[5] ANDERSOJN.D, . Jr. (1990) Modern Compressible Flow: With Historical Perspective, 2nd Edition (McGraw-Hill)
[6] E.N. Jacobs, K.E. Ward, & R.M. Pinkerton. NACA Report No. 460, "The characteristics of 78 related airfoil sections from tests in the variable-density wind tunnel". NACA, 1933.
[7] Aerospaceweb.org | Ask Us - NACA Airfoil Series
[8] Bansal AK, Zoolagud SS. Bamboo composites: material of the future. J Bamboo Rattan 2002
[9] Murphy RJ, Alvin KL. Variation in fibre wall structure in bamboo. IAWA Bull 1992
[10] Wong KJ, Zahi S, Low KO, Lim CC. Fracture characterization of short bamboo fibre reinforced polyester composites. Mater Des 2010
[11] Das M, Chakraborty D. Role of mercerization of the bamboo strips on the impact properties and morphology of unidirectional bamboo strips–Novolac composites. Polym Compos 2007
[12] Okubo K, Fujii T, Yamamoto Y. Development of bamboo-based polymer composites
[13] Ghoshal AK. Bamboo fibre reinforced polypropylene composites and their mechanical, thermal, and morphological properties. 2011
[14] Joshi SV, Drzal LT, Mohanty AK, Arora S. Are natural fibre composites environmentally superior to glass fibre reinforced composites 2004
[15] Reddy GR, Reddy HK. Flexural and compressive properties of bamboo and glass fibre-reinforced epoxy hybrid composites. J Reinf Plast Compos 2010;
[16] "1991 Yamaha FZ FZR600 Dyno Dynamometer Result Graph. N.d. Photograph. Drag TimesWeb. 25 Mar 2012. <www.dragtimes.com/1991-Yamaha-FZ-Dyno-Results- Graphs-8173.html>.
[17] http://www.aerodyndesign.com/PROP_10/PROP_10.htm